A Multi-Reflection-Point Target Model for Classification of Pedestrians by Automotive Radar

Eugen Schubert[1], Martin Kunert[1], Andreas Frischen[2], Wolfgang Menzel[3]

[1]Robert Bosch GmbH, Advanced Engineering Sensor Systems, P.O. Box 16 61, 71226 Leonberg, Germany
[2]Robert Bosch GmbH, Corporate Sector Research and Advance Engineering, Gerlingen, Germany
[3]Ulm University, Institute of Microwave Techniques, Ulm, Germany
Email: eugen.schubert@de.bosch.com

***Abstract*—Pedestrian Collision Mitigation Systems (PCMS) are in the market for a few years. Due to continuously evolving Euro NCAP regulations their presence will rapidly increase. Visual sensors, already capable of pedestrian classification, provide functional benefits because system responses can be better adapted to expected pedestrian's behavior. Nevertheless their performance will suffer under adverse environmental conditions like darkness, fog, rain or backlight. Even in such situations the performance of radar sensors is not significantly deteriorated. Enabling classification capability for radar-based systems will increase road safety further and will lower PCMS's overall costs. In this paper a multi-reflection-point pedestrian target model based on motion analysis is presented. Together with an appropriate sensor model, pedestrian radar signal responses can be provided for a wide range of relevant accident scenarios, without risk for the health of test persons. Besides determination of human classification features, the model provides identification of the limits in classical radar signal processing. Beyond these borderlines it offers the opportunity to evaluate parametric spectral analysis methods.**

Keywords— automotive radar; radar signal processing; spectral analysis

I. INTRODUCTION

According to the Euro NCAP Roadmap Pedestrian Collision Mitigation Systems (PCMS) will be evaluated as from 2016. Although modern PCMS will be able to handle these tests, improving the performance will still go on. Beyond the time frame of 2016 future PCMS will not just brake. Algorithms based on adaptive parameterized pedestrian tracking will be used to determine the most suitable emergency maneuver out of a diversity of mitigation strategies. Thereby, highest collision mitigation is achieved while simultaneously unjustified system interventions are prevented [1]. To adapt the tracking algorithms to several object classes, e.g. pedestrians, reliable classification algorithms are necessary. Because of its advantages compared to other sensing technologies, radar will be one of the essential sensor technologies in future PCMS. However one deficiency of the state of the art automotive radar sensors is still the lack of reliability in pedestrian classification. Addressing this functionality within future radar sensor generations will increase road safety especially under adverse weather conditions, like fog, rain or visual reflections of headlights on wet roads. The value of already existing safety functions will be increased by reliable classification of critical objects as pedestrians; because of a higher level of driver's acceptance of automatic interventions in situations pedestrians are involved. Additionally unjustified system responses will be suppressed. For instance the activation of an active bonnet only in case of an expected classified pedestrian impact will minimize maintenance effort and associated costs. First approaches in automotive radar-based pedestrian classification mostly rely on the evaluation of object's range and velocity spreads [3].

In this paper, a multipoint radar target model capable of simulating high resolution radar responses of pedestrian accident scenarios is presented. Detailed results of a well suited approach of motion analysis are discussed, followed by the description of development and integration of the target model in an automotive radar simulation environment. Finally simulation results of pedestrian accident scenarios and deduced features for pedestrian classification are presented. Additionally the impact of applying autoregressive spectral analysis to resolution and classification features is evaluated.

II. HUMAN MOTION ANALYSIS

Based on observations of pedestrians with a 24 GHz Pulse-Doppler radar, a six point model representing feet, knees and two points of the upper body is developed in [4]. Thereby the movements of the legs are approximated by sinusoidal oscillations in the direction of motion superimposed to the motion of the center of gravity (CoG). Swinging arms are neglected. A more detailed approach for pedestrian modeling to estimate human walking parameters is presented in [5]. Parameters, such as cycle frequency, cycle length or cycle phase are estimated and visualized with a human walking scene in virtual reality. In [6], high resolution 12.5 GHz inverse synthetic aperture radar (ISAR) is used for Doppler measurements of pedestrians. Human motion simulation and measurements are compared to define the constraints of image processing radar. Thereby 2D radar images were simulated from motion data partially obtained from [7] with respect of seven distinctive points (sternum, hands, knees, and toes). However, simulations of pedestrian accident scenarios are very rarely addressed in literature. Most existing target models underlay simplifications which could affect the deduction of classification features. Further on, observations of pedestrians in literature are often based on measurement principles, like SAR or UWB, that do not suitable match automotive requirements in terms of sensor size or available bandwidth.

In this work, a simple but well suited measurement setup is used to develop a pedestrian target model. Test persons, tagged at the feet (FR/FL), knees (KR/KL), hands (HR/HL), elbows (ER/EL), right shoulder, right hip and head (H), have been asked to walk in front of a grid, projected on a white wall. The motion sequences were recorded cinematically with a frame rate of up to 240 fps to obtain the space-time information of different body parts. Velocity-time functions have been derived through numerical differentiation and low pass filtering. Fig. 1a displays the measured space vs. time functions and Fig. 1b the speed vs. time functions of each body part. Because of the linear uniform movement of the head, its function is considered to be representative for the pedestrian's center of gravity. Closer looks at the speed-time-functions show that they do not follow an ideal sinusoidal character, as simple models in literature propose [4]. This must be kept in mind when pedestrians shall be realistically represented during system assessment by articulating dummies, capable of arm and leg movement. Different lengths of arms and legs result in different velocity amplitudes. Furthermore it is obvious from the records that the body parts are accelerated several times during one gait cycle. Thereby the feet reach the highest spread in the velocity domain of approximately three times the mean value. Caused by the rolling motion of the feet, their velocities reach zero only for a distinct amount of time while other body parts are in motion over the whole gait cycle. Caused by the cinematic measurement method the positions of the left body parts could not be measured continuously. Nevertheless the measured data are sufficient enough to prove the assumption that the shape of left and right extremities are identical with a phase shift of pi, as can be seen in the space time functions given in Fig. 1a.

For further investigations on the influence of the walking speed to the maximum velocity, step frequency and step length measurements of different paces of a person were done. Fig. 1c and Fig. 1d show the speed time functions of strolling and jogging motion. Characteristic values of the different speed-time-functions are listed in Table 1. Given the minor difference between the peak velocity during walking and jogging, the existence of an upper border for the peak velocity can be assumed. For faster paces the increased mean value is achieved rather by a broader shape of the curve than by the increase of the peak velocity. Furthermore, in case of faster movement, sinusoidal approximation of the velocity functions is nearly justifiable. The results gained with the approach presented are quite comparable to the findings of more sophisticated measurement methods of [6] and [7] and therefore highly suitable for simulation model development.

TABLE I. CHARACTERISTIC VALUES OF DIFFERENT PACES

	strolling	walking	jogging
v_{mean}[m/s]	0.95	1.43	2.20
v_{max} [m/s]	3.08	4.30	4.60
f_{step} [Hz]	0.75	0.97	1.20
s_{step}[m]	1.28	1.47	1.75

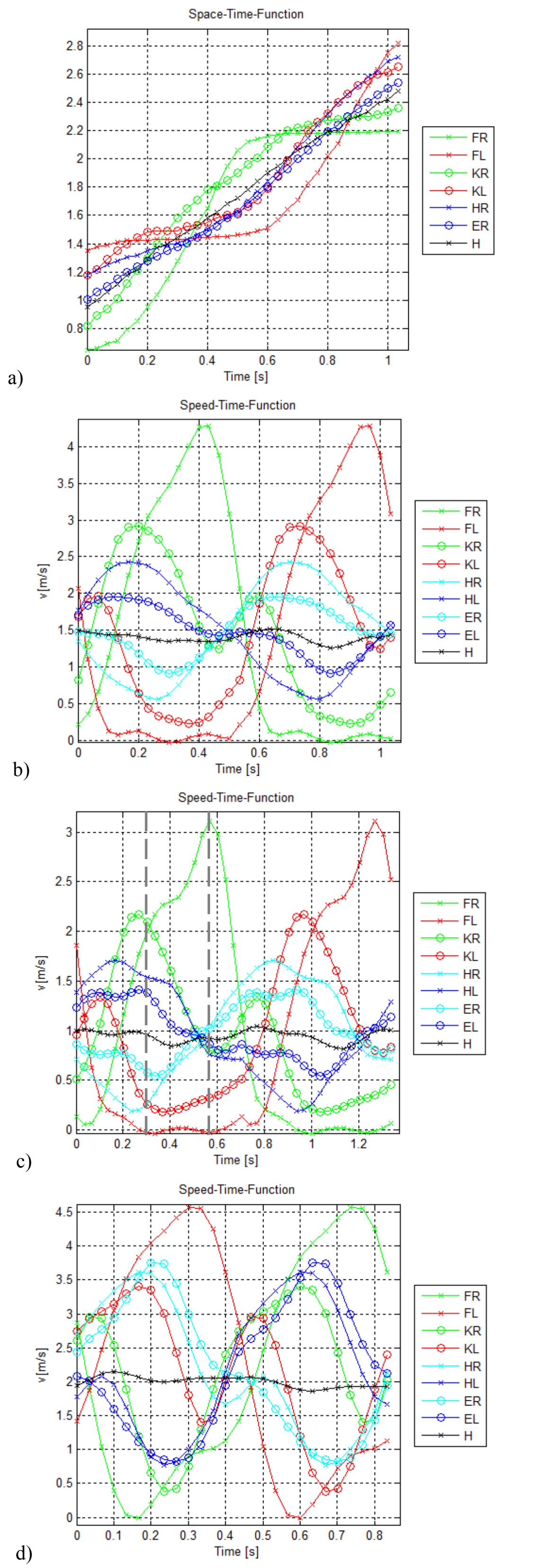

Fig. 1. Space-Time-Function of a walking pedestrian (a) and Speed-Time-Functions of a walking (b), strolling (c) and jogging (d) pedestrian (FR/FL:foot right/left, KR/KL: knee right/left, HR/HL: hand right/left, ER/EL elbow right/left, H: head)

III. SIMULATION ENVIRONMENT

A. Sensor Model

A sensor model featuring chirp sequence modulation provides the advantage of unambiguous range and velocity determination. The reflected and down converted signal of K consecutively transmitted frequently modulated continuous wave (FMCW) signals is described by

$$s_{IF}(t) = e^{j2\pi\left(\frac{2f_c\cdot R}{c_0}\right)} \cdot \sum_{k=0}^{K-1} e^{j2\pi\left[\frac{2f_c\cdot v_r\cdot T_{RRI}\cdot k}{c_0}+\left(\frac{2f_c\cdot v_r}{c_0}+\frac{2B\cdot R}{T\cdot c_0}\right)\cdot t\right]}\cdot rect\left(\frac{t-k\cdot T_{RRI}}{T}\right), \quad (1)$$

with single-chirp duration T, bandwidth B, carrier frequency f_c, chirp repetition interval TRRI, chirp number k, target's radial velocity v_r and distance d_r [8]. Consequently, the radar target model of the pedestrian must provide the radial range and velocity of all considered reflection points for each time step of a scenario. Characteristic values of the used modulation are given in Table II. These values ensure results with high resolution and excellent target separability.

TABLE II. MODULATION CHARACTERISTICS

Parameter	Value	Parameter	Value
f_c	76.5 GHz	cyclerate	20 Hz
B	500 MHz	Δv_r	0.15 ms^{-1}
T	20 µs	Δd_r	0.30m
TRRI	25 µs	$d_{r,max}$	153 m
K	512	$v_{r,max}$	40 ms^{-1}

B. Pedestrian Target Model

To determine analytical velocity vs. time and space vs. time functions of each reflection point of the pedestrian target model, the measured data of Fig. 1 were processed by a FFT. Each velocity function can be represented by the sum of a small amount of oscillations depending on sample frequency of the camera f_0 and the set of complex Fourier coefficients c_k.

$$v(t) = \frac{c_{mean}}{c_0} \cdot \sum_{k=-\infty}^{\infty} c_k e^{j2\pi k f_0 t} \quad (2)$$

To compensate slight measurement uncertainties the steady components are rescaled to a common mean value c_{mean}, corresponding to v_{mean} of Table I. Integration of (2) results in space-time functions

$$s(t) = c_{mean} \cdot t + \sum_{k=-\infty/0}^{\infty} \frac{c_{mean}}{c_0} \frac{c_k}{j2\pi k f_0}\left(e^{j2\pi k f_0 t} - 1\right) + s_0 \quad (3)$$

of the different body parts. Thereby the integration constant was replaced by the position offsets (s_0) between the center of gravity and each body part at the beginning of the cycle. Given (2) and (3) and the parameter set of c_k enables the simulation of a multiple point pedestrian motion model for any desired time length. In the last step the functions were converted into radial coordinate system of the sensor model and included in the Matlab-based simulation environment. By providing adjustable parameters such as starting point, direction angle, vehicle velocity and simulation duration, this environment enables the simulation of radar responses of nearly all relevant accident scenarios without the need to run dangerous or life-threatening real-world tests.

To provide highly realistic radar responses the different reflection points of the human body feature different Radar Cross Section (RCS) values. The signal levels are approximated by combining the mean RCS value of a pedestrian in 76 GHz band of –6.6 dBsm [2] with the partial distribution of the body surface according to [9]. The RCS used for the different body parts are listed in Table III.

TABLE III. RCS VALUES OF REFLECTION POINTS

Reflection-Point	FR/FL	KR/KL	HR/HL	ER/EL	CoG
RCS [dBsm]	-20.7	-14.2	-23.6	-18.6	-10.4

To verify the developed model measurements in the 5.8 GHz band were performed in an anechoic chamber. With 1024 frequency chirps per cycle and a duration of T=256µs each the velocity resolution follows to be 0.1m/s. Fig. 2 shows the simulated (a) and measured (b) Range-Doppler (RD) response of a 260ms long motion segment of a radial walking pedestrian comparable to the segment indicated by the two thicker dashed lines of Fig. 1c. Beside ground clutter presence and minor RCS differences, both RD responses show very similar distribution of velocities. This confirms the main assumptions made in the simulation model.

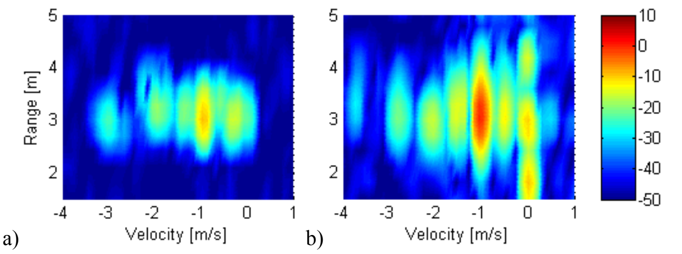

Fig. 2. Simulated (a) and measured (b) RD response of a walking pedestrian

IV. ACCIDENT SCENARIO SIMULATION

A deeper look at the distribution of accident scenarios shows, that pedestrian accidents in real world happen not exclusively in scenarios proposed by Euro NCAP tests. A significant amount of accidents with killed or serious injured pedestrians occur also in additional scenarios like: "Along the carriageway on a straight road without obstruction" (Fig. 3a) [10]. A system capable to indicate the presence of pedestrians under adverse visibility conditions, like rain, fog or darkness in combination with wet roads and related reflecting backlight, may be an easy entry of radar-based pedestrian classification into the market. An automatic triggered pedestrian warning enables the driver to faster adapt his driving behavior to the situation and help to avoid a potential safety-critical situation.

For a deeper analysis of the classification potential, Fig. 4 provides simulated RD responses of different scenarios cumulated over successive sequences. A comparison between Fig. 4a and Fig. 4b shows the possibility to discriminate a longitudinal walking pedestrian from a static reflection by evaluating the velocity distribution - several seconds before a collision may occur. Especially scenarios with lateral moving pedestrians and high vehicle velocities, as illustrated in Fig. 3b, are challenging for radar-based pedestrian classification, because of smaller angles and smaller radial components of the velocities. Fig. 4c shows the RD responses cumulated over time of a laterally moving pedestrian. Even if some differences can be recognized by comparing the shapes of Fig. 4a and Fig. 4c, separation of reflection points by their velocities is not reliably possible, even with a velocity separability of $0.3 ms^{-1}$ (twice the resolution given in Table II).

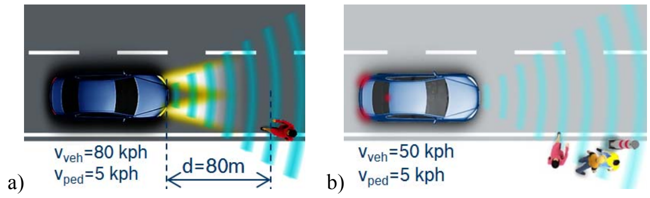

Fig. 3. Accident scenarios along carriageway during darkness (a) and crossing pedestrian in an urban area (b)

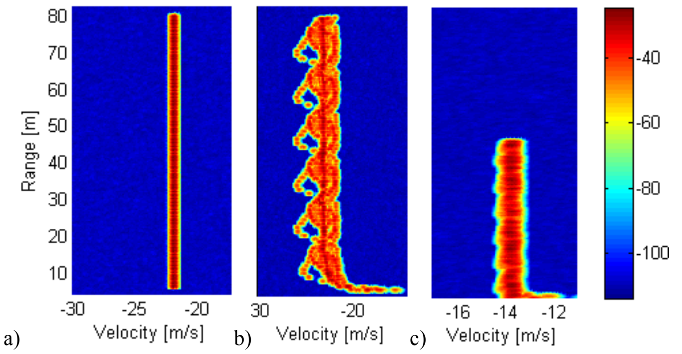

Fig. 4. RD responses cumulated over time for different scenarios: (a) approaching stationary target with 80km/h and intial distance of 80m; (b) approaching longitudinally walking pedestrian with 80km/h and intial distance of 80m; (c) crossing pedestrian on collision course and v_{veh}=50 km/h

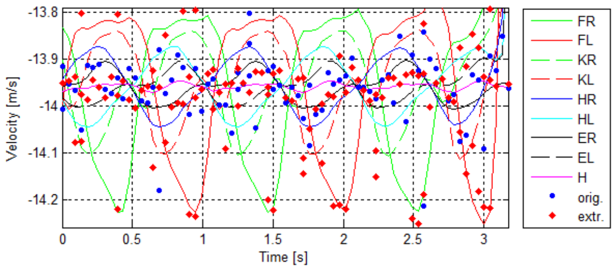

Fig. 5. Detections based on simulated signal (blue dots) and based on the extended simulated signal (red dots) vs. time of the crossing pedestrian scenario in comparision to the model based velocity functions

Fig. 5 illustrates the detections over time (blue dots) derived after applying CFAR and peak detection of each simulated cycle in comparison to the velocity functions of the pedestrian motion model. Distinct separation of the individual body parts is not possible within most cycles, but a wide spread of the detected velocities around their mean value can be still recognized over time. This is caused by the different RCS of the body parts and the fact that radar backscatter always respond the superposition of non resolvable reflection points. Evaluation of the velocity's variance over time is also appropriate for classification of pedestrians in case of poor separability. A deeper look to the simulations lets us assume that a separability of at least $0.2 ms^{-1}$ is needed to separate a minimum of two prominent reflections at least at some points of the gait cycle. Improvement of the velocity separation requires in general extending the measurement time and leads to a decreased cycle rate of the sensor. Linear prediction algorithms may offer solutions for this dilemma. Thereby filter coefficients were estimated from the measured signal by the Burg algorithm and used by a linear filter to extrapolate simulated baseband signals. This allows application of larger window and FFT sizes and consequently a gain in resolution and separability can be achieved. Fig. 5 also allows a comparison of the detections of the original, 512 samples long, signal (blue dots) and of the extrapolated, 1024 samples long, signal (red rhombuses). Doubling the number of samples increases the separation from $0.3 ms^{-1}$ to $0.15 ms^{-1}$ and enables separation especially of the legs and feet from the body. This offers the possibility of single snapshot classification at least at the times of gait cycle when feet reach maximum velocity.

V. Conclusion

Starting with a detailed pedestrian motion analysis a multi-reflection-point target model was developed to simulate radar reflection characteristics of a pedestrian in relevant accident scenarios. Based on these, radar resolution requirements for pedestrian classification were derived. Additionally, the captured motion data provided in this paper can be further used to specify articulating dummies for system testing.

Because velocity resolution is proportional to measurement time, which is limited by cycle rate requirements, the potential of linear prediction signal processing to increase the separability in the velocity domain was presented. Results based on simulated data are auspicious and will be undergo a deeper validation in near future, especially to determine limitations of the used algorithm.

References

[1] C. Bräuchle, F. Flehmig, W. Rosenstiel, T. Kropf, "Maneuver decision for active pedestrian protection under uncertainty", IEEE Annual Conference on Intelligent Transportation Systems, Netherlands, 2013

[2] E. Schubert, M. Kunert, W. Menzel, J. Fortuny-Guasch, J.-M. Chareau, "Human RCS measurements and dummy requirements for the assessment of radar based active pedestrian safety systems", 14th International Radar Symposium (IRS), Dresden, Germany, 2013

[3] H.Rohling, S. Heuel, H. Ritter, "Pedestrian detection procedure integrated into an 24 GHz automotive radar", IEEE International Radar Conference (RADAR2010), Washington DC, USA, May 2010

[4] F.Fölster, H.Rohling, H.Ritter , "Observation of a walking pedestrian with a 24GHz automotive radar sensor", GeMIC, 2006

[5] P. v. Dorp, F.C.A. Groen, "Human walking estimation with radar", IEE Proceedings Radar, Sonar & Navigation, Oct. 2003, Vol. 150, Issue 5, pp. 356-365

[6] A. Ghaleb, L. Vignaud, J.M. Nicolas, "Micro-Doppler analysis of wheels and pedestrians in ISAR imaging", IET Signal Processing, Volume 2, Issue 3, pp.301-311, 2008

[7] Motion Capture Database of Carnegie Mellon University Graphics Lab, Pittsburgh, PA 15213, http://mocap.cs.cmu.edu

[8] M. Andres, W. Menzel, H.-L. Bloecher, J. Dickmann, "Detection of slow moving targets using automotive radar sensors", GeMIC 2012

[9] E.H. Livingston, S. Lee, "Body surface area prediction in normal-weight and obese patients", American Journal of Physiology - Endocrinology and Metabolism, 2001, Vol. 281 no. E586-E591

[10] M. Wisch et al., "Scenarios and weighting factors for pre-crash assessment of integrated pedestrian safety systems", EU FP7 ASPECSS Deliverable 1.1, Ch. 5, p.59, 2013, http://www.aspecss-project.eu